The Astrophysical Journal, 837:1 (8pp), 2017 March 1 https://doi.org/10.3847/1538-4357/aa5f57
© 2017. The American Astronomical Society. All rights reserved.

Broad-lined Supernova 2016coi with a Helium Envelope

Masayuki Yamanaka[1], Tatsuya Nakaoka[2], Masaomi Tanaka[3], Keiichi Maeda[4,5], Satoshi Honda[6], Hidekazu Hanayama[7], Tomoki Morokuma[8], Masataka Imai[9], Kenzo Kinugasa[10], Katsuhiro L. Murata[11], Takefumi Nishimori[12], Osamu Hashimoto[13], Hirotaka Gima[12], Kensuke Hosoya[6], Ayano Ito[12], Mayu Karita[6], Miho Kawabata[2], Kumiko Morihana[6], Yuto Morikawa[12], Kotone Murakami[12], Takahiro Nagayama[12], Tatsuharu Ono[14], Hiroki Onozato[15], Yuki Sarugaku[16], Mitsuteru Sato[17], Daisuke Suzuki[18], Jun Takahashi[6], Masaki Takayama[6], Hijiri Yaguchi[6], Hiroshi Akitaya[2,19], Yuichiro Asakura[20], Koji S. Kawabata[2,19], Daisuke Kuroda[21], Daisaku Nogami[4], Yumiko Oasa[22], Toshihiro Omodaka[12], Yoshihiko Saito[23], Kazuhiro Sekiguchi[3], Nozomu Tominaga[1,5], Makoto Uemura[2,19], and Makoto Watanabe[24]

[1] Department of Physics, Faculty of Science and Engineering, Konan University, Okamoto, Kobe, Hyogo 658-8501, Japan; yamanaka@center.konan-u.ac.jp
[2] Department of Physical Science, Hiroshima University, Kagamiyama 1-3-1, Higashi-Hiroshima 739-8526, Japan
[3] National Astronomical Observatory of Japan, National Institutes of Natural Sciences, Osawa, Mitaka, Tokyo 181-8588, Japan
[4] Department of Astronomy, Graduate School of Science, Kyoto University, Sakyo-ku, Kyoto 606-8502, Japan
[5] Kavli Institute for the Physics and Mathematics of the Universe (WPI), The University of Tokyo, 5-1-5 Kashiwanoha, Kashiwa, Chiba 277-8583, Japan
[6] Nishi-Harima Astronomical Observatory, Center for Astronomy, University of Hyogo, 407-2 Nishigaichi, Sayo-cho, Sayo, Hyogo 679-5313, Japan
[7] Ishigakijima Astronomical Observatory, National Astronomical Observatory of Japan, National Institutes of Natural Sciences, 1024-1 Arakawa, Ishigaki, Okinawa 907-0024, Japan
[8] Institute of Astronomy, Graduate School of Science, The University of Tokyo, 2-21-1 Osawa, Mitaka, Tokyo 181-0015, Japan
[9] Department of Cosmosciences, Graduate School of Science, Hokkaido University, Kita 10 Nishi8, Kita-ku, Sapporo 060-0810, Japan
[10] Nobeyama Radio Observatory, National Astronomical Observatory of Japan, National Institutes of Natural Sciences, 462-2 Nobeyama, Minamimaki, Minamisaku, Nagano 384-1305, Japan
[11] Department of Astrophysics, Nagoya University, Chikusa-ku, Nagoya 464-8602, Japan
[12] Graduate School of Science and Engineering, Kagoshima University, 1-21-35 Korimoto, Kagoshima 890-0065, Japan
[13] Gunma Astronomical Observatory, Takayama, Gunma 377-0702, Japan
[14] Earth and Planetary Sciences, School of Science, Hokkaido University, Kita 10 Nishi8, Kita-ku, Sapporo 060-0810, Japan
[15] Astronomical Institute, Graduate School of Science, Tohoku University, 6-3 Aramaki Aoba, Aoba-ku, Sendai, Miyagi, 980-8578, Japan
[16] Kiso Observatory, Institute of Astronomy, Graduate School of Science, The University of Tokyo, Mitake, Kiso machi, Kiso, Nagano 397-0101, Japan
[17] Faculty of Science, Hokkaido University, Kita 10 Nishi8, Kita-ku, Sapporo 060-0810, Japan
[18] Code 667, NASA Goddard Space Flight Center, Greenbelt, MD 20771, USA
[19] Hiroshima Astrophysical Science Center, Hiroshima University, Higashi-Hiroshima, Hiroshima 739-8526, Japan
[20] Institute for Space-Earth Environmental Research, Nagoya University, Furocho, Chikusa-ku, Nagoya, 464-8601, Japan
[21] Okayama Astrophysical Observatory, National Astronomical Observatory of Japan, National Institutes of Natural Sciences, 3037-5 Honjo, Kamogata, Asakuchi, Okayama 719-0232, Japan
[22] Faculty of Education, Saitama University, 255 Shimo-Okubo, Sakura, Saitama, 338-8570, Japan
[23] Department of Physics, Tokyo Institute of Technology, 2-12-1 Ookayama, Meguro-ku, Tokyo 152-8551, Japan
[24] Department of Applied Physics, Okayama University of Science, 1-1, Ridai-cho, Kita-ku, Okayama, Okayama 700-0005, Japan
Received 2016 August 19; revised 2017 February 2; accepted 2017 February 4; published 2017 February 27

Abstract

We present the early-phase spectra and the light curves of the broad-lined (BL) supernova (SN) 2016coi from $t = 7$ to 67 days after the estimated explosion date. This SN was initially reported as a BL Type SN Ic (SN Ic-BL). However, we found that spectra up to $t = 12$ days exhibited the He I λ5876, λ6678, and λ7065 absorption lines. We show that the smoothed and blueshifted spectra of normal SNe Ib are remarkably similar to the observed spectrum of SN 2016coi. The line velocities of SN 2016coi were similar to those of SNe Ic-BL and significantly faster than those of SNe Ib. Analyses of the line velocity and light curve suggest that the kinetic energy and the total ejecta mass of SN 2016coi are similar to those of SNe Ic-BL. Together with BL SNe 2009bb and 2012ap, for which the detection of He I was also reported, these SNe could be transitional objects between SNe Ic-BL and SNe Ib, and be classified as BL Type "Ib" SNe (SNe "Ib"-BL). Our work demonstrates the diversity of the outermost layer in BL SNe, which should be related to the variety of the evolutionary paths.

Key words: supernovae: general – supernovae: individual (SN 2016coi, SNe 1998bw, 2008D, 2009bb, 2012au)

1. Introduction

Core-collapse supernovae (SNe) are classified as Type Ib when the spectra exhibit helium but not hydrogen, while SNe are classified as Type Ic when the spectra exhibit neither helium nor hydrogen (Filippenko 1997). The absorption lines reflect the compositions of the outer layers of the SN ejecta and progenitor. It is known that properties of SNe Ib/c have a large variety. Some SNe Ib/c show broad absorption features, and such objects are called broad-lined (BL) SN Ic (SN Ic-BL; Valenti et al. 2008). The high expansion velocities suggest that SNe Ic-BL have a higher energy than normal SNe Ib/c (Foley et al. 2003; Valenti et al. 2008). SNe Ic-BL associated with a γ-ray burst (GRB-SNe) form a particularly missing subclass (Galama et al. 1998; Iwamoto et al. 1998). Their kinetic energy is likely to be even larger than those of other SNe Ic-BL (Nomoto et al. 2006). The origin of these varieties, however, is not well understood yet.

In theoretical models of stellar evolution, it is not straightforward to produce SN progenitors with no He layer. The stellar wind and binary interaction play important roles in removing the envelope. Interestingly, even in binary models, which are probably favored over single-star models in removing the envelope, the progenitors tend to have some

helium layer (Woosley et al. 1995; Yoon et al. 2010; Yoon 2015). Thus, to study the evolutionary paths to GRB-SNe and SNe Ic-BL, it is important to observationally probe the presence of He in these classes of SNe.

Due to the relatively low event rate, the direct detection of the progenitor of SNe Ic-BL has not been reported to date. Thus, it is important to study the composition of the progenitor star from the early-phase spectra of SNe. In fact, the presence of the He features in optical and near-infrared (NIR) spectra of SNe Ic-BL has been suggested for SNe 2009bb and 2012ap (Pignata et al. 2011; Bufano et al. 2012; Milisavljevic et al. 2015). For SN 2009bb, however, the identification is based mainly on the He I λ5876 line, which could be contaminated by the Na I D line (Pignata et al. 2011). In the spectra of SN 2009bb, the He Iλ6678 and λ7065 lines were very weak. For SN 2012ap, the strong He I λ10830 line was detected, but the He I λ20587 line, which is expected to have a similar strength to the He I λ10830, was weak (Milisavljevic et al. 2015). Also, a statistical analysis of spectra of SNe Ic and SNe Ic-BL has been done by Modjaz et al. (2016). They reported that these types of SNe do not show detectable helium absorption lines. In sum, the presence of the He layer in SNe Ic and Ic-BL is still controversial.

In this paper, we present the results of our observations of SN 2016coi. SN 2016coi was discovered in the outskirts of the nearby faint galaxy UGC 11868 on May 27.5 by the ASAS-SN team (Holoien et al. 2016). The name of this SN was independently given as ASASSN-16fp. The distance of the host galaxy was obtained to be 17.2 Mpc using Tully–Fisher relation.[27] Follow-up spectroscopic observations were performed by several groups and the spectra were very similar to those of SNe Ic-BL in their early phase (Elias-Rosa et al. 2016).

We first describe our observations and data reduction in Section 2. In Section 3, we compare the properties with those of SNe Ib and Ic-BL. We show that the spectral properties of SN 2016coi were very similar to those of SNe Ic-BL except for the detection of the He I absorption lines. This suggests that SN 2016coi is a transitional SN between SNe Ib and Ic-BL, and could be classified as an SN "Ib"-BL. Finally, we discuss the explosion properties and progenitor nature of SN 2016coi in Section 4.

2. Observations and Data Reduction

Observations of SN 2016coi were performed using various telescopes and instruments in the framework of the Target-of-Opportunity program in the Optical and Infrared Synergetic Telescopes for Education and Research. Optical spectroscopic observations were performed using the 1.5 m Kanata telescope attached to the Hiroshima One-shot Wide-field Polarimeter (HOWPol; Kawabata et al. 2008) on 14 nights from May 31 through July 4. Spectroscopic observations were also performed using the 1.5 m telescope attached to the Gunma Low-resolution Spectrograph and imager (GLOWS) on three nights from June 2 through June 17, and the 2.0 m Nayuta telescope attached to the Medium- and Low-dispersion Long-slit Spectrograph (MALLS) on four nights from June 2 through July 2.

Spectroscopic data were reduced according to the standard manner. Wavelength calibrations were performed for the HOWPol data using atmospheric lines observed in the same frame as the object, and for the GLOWS and the MALLS data using the FeNeAr lamp. Flux calibrations were performed using bright high-temperature standard stars. The atmospheric lines of the SN spectra were corrected for using the standard-star spectra.

Optical imaging observations were performed using the Kanata telescope attached to the HOWPol on 17 nights from May 31 through July 26, the 1.6 m Pirka telescope attached to the Multispectral Imager (MSI; Watanabe et al. 2012) on 21 nights from June 2 through July 25, the 1.05 m telescope attached to the Kiso Wide Field Camera (KWFC; Sako et al. 2012) on six nights from June 2 through June 17, and the 1.05 m telescope in the Multicolor Imaging Telescopes for Survey and Monstrous Explosions (MITSuME; Kotani et al. 2005) at the Ishigakijima Astronomical Observatory on 28 nights from June 3 through July 30. Imaging observations of photometric standard star fields were also performed using the HOWPol and the MSI on photometric nights. NIR photometry was performed using the 1.4 m Infrared Survey Facility (IRSF) telescope attached to the Simultaneous Three-color Infrared Imager for Unbiased Survey (SIRIUS; Nagayama et al. 2003) on June 3, the Kanata telescope attached to the Hiroshima Optical and NIR camera (HONIR; Sakimoto et al. 2012; Akitaya et al. 2014; Ui et al. 2014) on June 1, the Nayuta telescope attached to the Nishi-harima Infrared Camera on June 14, and the 1.0 m telescope at Kagoshima University on four nights from June 14 through July 21.

Reductions of the imaging data were performed with similar methods to previous studies (see Yamanaka et al. 2015, 2016). The point-spread function photometry was performed using the IRAF software DAOPHOT. Standard magnitudes of the local standard stars were obtained using the standard star magnitudes (Landolt 1992). Systematic differences among different instruments were confirmed. We corrected for the color terms of HOWPol (Kawabata et al. 2008), MSI (Watanabe et al. 2012), KWFC (Sako et al. 2012), and MITSuME (Kotani et al. 2005) when SN magnitudes were calculated. The color terms of these instruments were already obtained using the secondary standard stars in M67 (see also Yamanaka et al. 2015, 2016). The systematic errors were calculated using the average of the residual differences.

The extinctions were corrected only for Galactic dust (Schlafly & Finkbeiner 2011). This is supported by the fact that the sodium absorption lines only from our Galaxy were detected in the spectra. The total extinction of $A_V = 0.2$ (Schlafly & Finkbeiner 2011) is adopted throughout this paper. The extinction coefficient is assumed to be $R_V = 3.1$ as a typical value.

3. Results

3.1. Spectral Features

Figure 1 shows the spectral evolution of SN 2016coi from $t = 7$ to 41 days.[28] The corrected redshift is $z = 0.0036$ for SN 2016coi. The spectra exhibited strong absorption lines around 6000 Å. The feature was identified as SiII λ6355 and its velocity reached 18,000 km s^{-1}. The broad absorption line around at 8000 Å was blended with the O I λ7774 and Ca II IR

[27] The distance was taken from the NASA/IPAC Extragalactic Database (NED), https://ned.ipac.caltech.edu/.

[28] $t = 0$ is the estimated explosion date and defined as MJD 57532.5. See Section 3.3 for details.

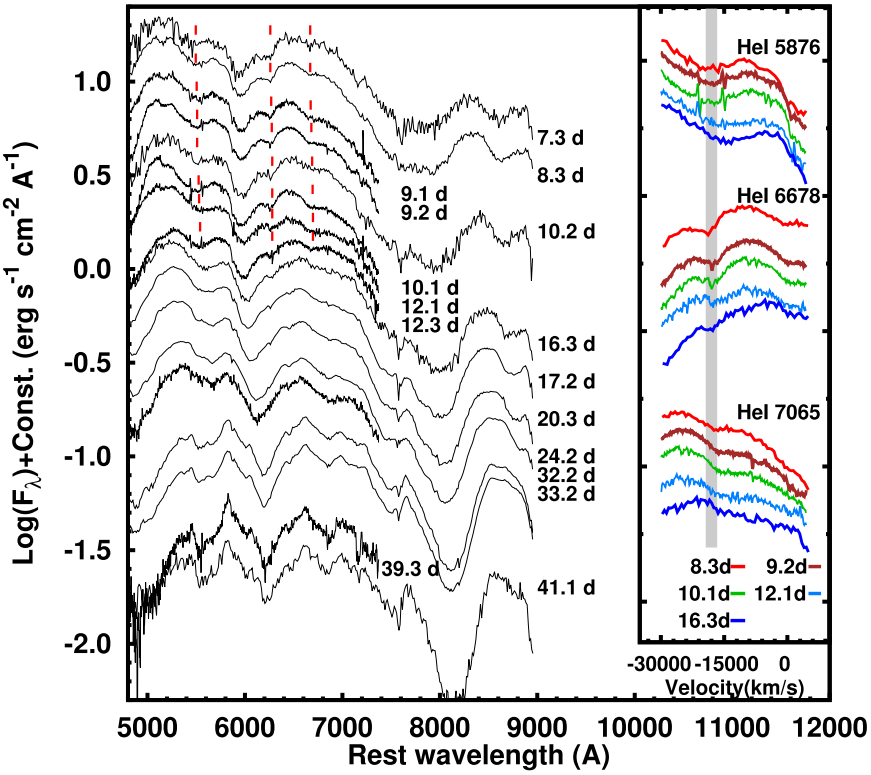

Figure 1. Spectral evolution of SN 2016coi from $t = 7$ to 41 days. Wavelengths of spectra were corrected for using the recession velocity of the host galaxy UGC 11868 ($z = 0.0036$; Giovanelli & Haynes 1993). Spectra were corrected for atmospheric lines using the spectrophotometric standard star spectra. Right inset: close-up view of the He Iλ5876, λ6678, and λ7065 regions shown in the Doppler velocity. The vertical gray line shows a velocity of 18,000 km s^{-1}.

triplet because of their extremely high velocities. Features marked by the red lines were attributed to He I. Identification of He I will be discussed in Section 3.2.

The spectrum at $t = 8$ days was compared with those of SNe Ic-BL 1998bw (Patat et al. 2001), 2002ap (Kawabata et al. 2002; Foley et al. 2003), and SN Ib 2008D (Modjaz et al. 2009) (see the top panel of Figure 2). The intensity of the Si II λ6355 absorption line of SN 2016coi was significantly stronger than in other SNe. Although the absorption depth generally becomes shallower when the feature is broadened as seen in SN 1998bw, the absorption line of SN 2016coi was deep and broad.

The broad feature around 7400–8200 Å could not be separated into different lines. This characteristic is common in SNe Ic-BL. For SN 1998bw, the Ca II IR triplet was blueshifted to ~7000 Å due to its extremely high-velocity ejecta and the feature was even blended with O I λ7774 (Tanaka et al. 2007). For SN 2002ap, the feature was dominated by O I only (Kawabata et al. 2002; Foley et al. 2003).

For the comparison of the spectrum at $t = 17$ days, the spectra of SN Ic-BL 2009bb (Pignata et al. 2011) and SN Ib 2012au (Takaki et al. 2013) were added (see the bottom panel of Figure 2). The line velocity of Si II λ6355 was similar to those of SNe Ic-BL 1998bw and 2009bb (see also the middle panel of Figure 3), but significantly faster than those of SNe Ib 2008D and 2012au. The broad feature composed of the O I and Ca II lines was still seen at this epoch. This feature was also similar to those of SNe 1998bw and 2009bb. The same feature in SN 2012au was completely separated into the O I and Ca II lines. In summary, SN 2016coi is similar to an SN Ic-BL in many respects. However, as discussed below, strong He I features were detected and the intensities were anomalously strong for SNe Ic-BL. With the spectra exhibiting He I, this SN should be classified as an SN "Ib"-BL according to the definition.

3.2. Detection of He I

Spectra up to $t = 12$ days exhibited absorption lines at 5500, 6300, and 6850 Å (see the inset of Figure 1). In this section, we show that these features were attributed to the absorption lines of He I λ5876, λ6678, and λ7065. The velocities reached 18,000 km s^{-1}, and the corresponding wavelengths were indicated by the vertical gray lines in Figures 1 and 2.

In order to confirm the line identification of He I, we first produced artificially smoothed spectra of SN Ic 2007gr (Yamanaka et al. 2016) and SN Ib 2012au (see Figure 4). We smoothed the spectra by using a Gaussian kernel so that the FWHM of absorption lines of SN 2016coi (11,000 km s^{-1}) matches to those of SNe 2007gr (5000 km s^{-1}) and 2012au (7500 km s^{-1}). Then, the spectra were further blueshifted to match the positions of the absorption lines. As shown in Figure 4, the spectrum of SN 2016coi was very similar to the smoothed and blueshifted spectrum of SN 2012au. We confirmed that in addition to the He I λ5876 line, both the He I λ6678 and λ7065 features were similar in the spectrum of SN 2016coi and the smoothed and blueshifted spectrum of SN 2012au. On the other hand, as expected from Type Ic identification, the smoothed and blueshifted spectrum of SN 2007gr did not exhibit the He I absorption lines. These tests demonstrate that SN 2016coi shows the He lines.

The relative absorption depths of the He lines were slightly different in SNe 2016coi and 2012au. We thus further study the

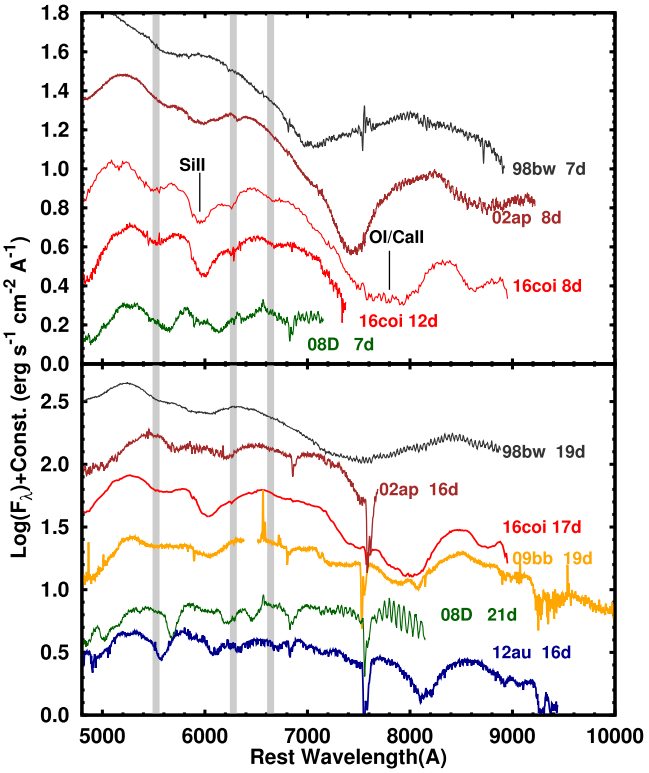

Figure 2. Top panel: spectra of SN 2016coi at $t = 8$ and 12 days compared with those of SNe Ic-BL 1998bw (Patat et al. 2001), 2002ap (Foley et al. 2003), and SN Ib 2008D (Modjaz et al. 2009). These data were taken from the SUSPECT[1] and WISEREP[2] databases. Vertical gray lines indicate the wavelength the He I λ5876, λ6678, and λ7065 lines, which were blueshifted by 18,000 km s^{-1}. Bottom panel: the spectrum at $t = 17$ days compared with those of other SNe as in the top panel as well as SNe 2009bb (Pignata et al. 2011) and 2012au (Takaki et al. 2013).

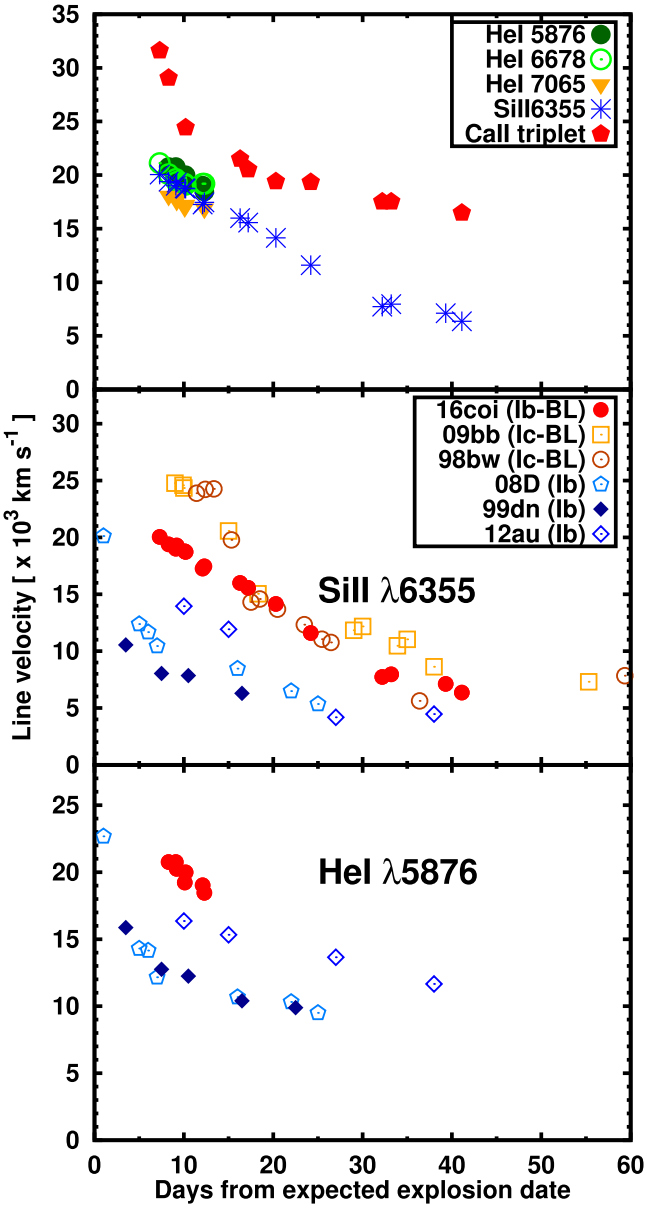

Figure 3. Top panel: velocity evolutions of Si IIλ6355, Ca II IR triplet, He Iλ7065, λ6678, and λ5876 lines. These line velocities were estimated from the absorption minimum measured using the *splot* task provided by IRAF. Middle panel: the line velocities of the Si II λ6355 line compared with those of SNe Ic-BL 1998bw, 2009bb, SNe Ib 1999dn, 2008D, and 2012au. Bottom panel: similar to the middle panel, but for the He I λ5876 line.

possible He I features of SN 2016coi using the synthetic spectral code SYN++ to assess possible contamination of the other lines in the He features. (Thomas et al. 2011). O I, Na I, Si II, Si III, Ca II, Fe II, and Co II were used to reproduce the depth ratio. Figure 5 shows that the Na ID and Si III features would contaminate the broad line at 5600 Å. The Co II $\lambda\lambda$5914, 6019 lines help to explain the strength of the feature at 5600 Å. The Co II $\lambda\lambda$6540, 6570 lines also support the explanation of the strong absorption line at 6200 Å (see Figure 5). The absorption lines at 5600, 6200, and 6600 Å were well explained using these components. On the other hand, it is hard to explain the depth ratios without He I lines (see Figure 5).

Note that inclusion of Co II at 3800 Å and 4400 Å and of other elements is also consistent with a blue portion of the spectrum. Since Fe-group elements strongly affect the spectra at ultraviolet wavelengths, we calculated $U - B$ color in the synthetic spectrum. The calculated color ($U - B = 0.6$ mag) is consistent with observed $U - B$ within the error. The Mg II and Ti II features possibly contribute to the spectra below 4500 Å, but again the U-band flux was consistent with the observed color even including these features.

To study the validity of our spectral fit, we also fit a spectrum of SN 2012au using the same ion species (He I, C I, O I, Na I, Si II, Si III, Ca II, Fe II, and Co II). The spectrum could be explained by the synthetic one except for slight differences at 6200 and 6600 Å. The absorption features of He I were well matched. This suggests that the Co II features could help to improve the spectral fit.

In summary, we identified He features in the pre-maximum spectra of SN 2016coi. The detection of He lines has been suggested in other SNe Ic-BL. The identification of He I has been discussed for SN Ic-BL 2009bb (Pignata et al. 2011). In SN 2009bb, the He I λ6678 and He I λ7065 features were very weak and the identification was marginal (see Figure 2). The NIR spectrum for SN 2012ap exhibited a strong absorption line around 10500 Å (Milisavljevic et al. 2015). The NIR and optical features were simultaneously explained using the synthetic spectra, but the authors pointed out that the He I λ20587 feature was too weak to explain the strength of He I λ10830 (see also Bufano et al. 2012). Compared with these two previous cases, the early-phase spectrum of SN 2016coi gives a more robust identification of the He I lines,

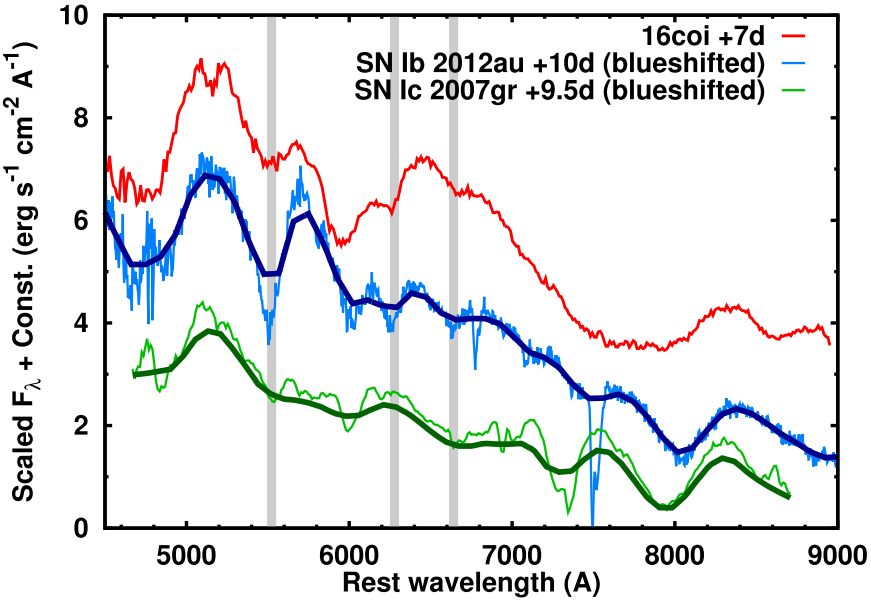

Figure 4. The spectrum of SN 2016coi at $t = 7$ days compared with the smoothed and blueshifted spectra of SN Ic 2007gr (Yamanaka et al. 2016) and SN Ib 2012au. The flux intensities of these two SNe were artificially scaled for the comparison. The degree of blueshift is determined to match the He I absorption lines of SN 2016coi. Gaussian kernel smoothing was also performed for these two SNe to match the width of He I absorption lines of SN 2016coi. The vertical lines indicate the He I absorption lines at their velocity of 18,000 km s^{-1}.

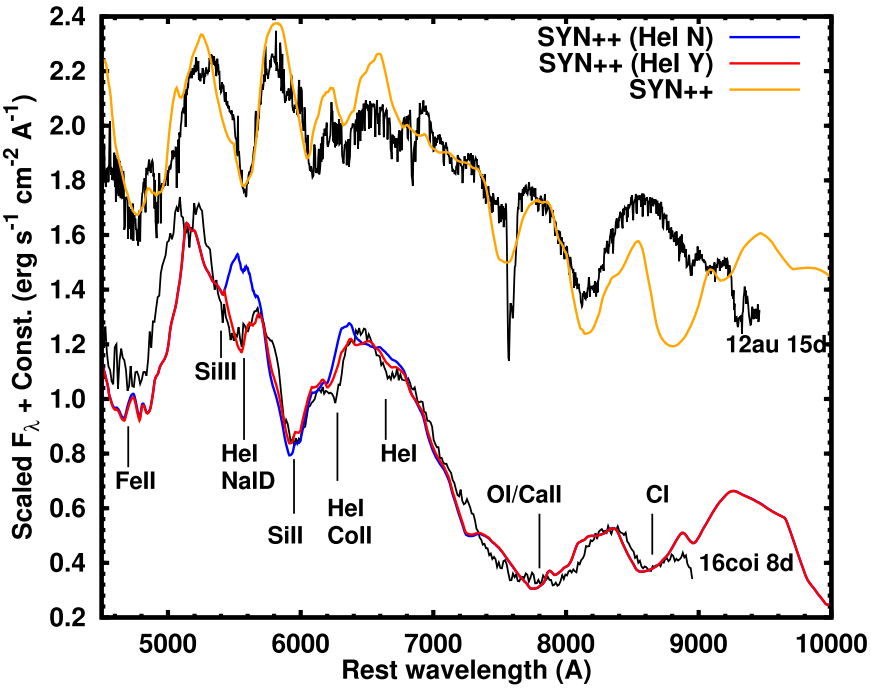

Figure 5. The observed spectrum of SN 2016coi at $t = 8$ days compared with the synthetic spectrum constructed using SYN++ (Thomas et al. 2011). The He I, C I, O I, Na I, Si II, Si III, Ca II, Fe II, and Co II features were used to calculate the spectrum. The synthetic spectrum without any He I feature is also presented.

because the lines were stronger than those of SNe 2009bb and 2012ap.

The bottom panel of Figure 3 shows a comparison of the He I λ5876 line velocities with those of SNe Ib 1999dn (Benetti et al. 2011), 2008D, and 2012au. The He velocity of SN 2016coi was almost identical to that of Si II λ6355, and was the fastest among other SNe Ib until $t = 12$ days. Again, the Si II λ6355 line velocity of SN 2016coi was very similar to those of SNe 1998bw and 2009bb after $t = 15$ days. These facts support the idea that SN 2016coi could be classified as an SN "Ib"-BL.

3.3. Light Curves

Figure 6 shows the multiband light curves of SN 2016coi. The V-band light curve showed a fast rise in the first two data points. By extrapolating the rising part, the explosion date was estimated to be MJD 57532.5 (May 24.5). This is consistent with the upper-limit magnitude reported by

[1] https://www.nhn.ou.edu/~suspect/
[2] http://wiserep.weizmann.ac.il/; (Yaron & Gal-Yam 2012).

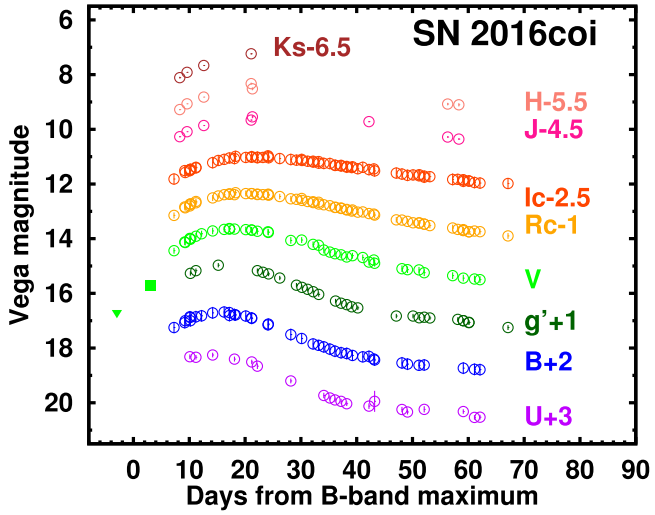

Figure 6. *UBg′VRIJHKs*-band light curves of SN 2016coi. The explosion date was estimated to be MJD 57532.5 ($t = 0$) by extrapolating the rising part. The triangles indicate the upper limit reported in Holoien et al. (2016).

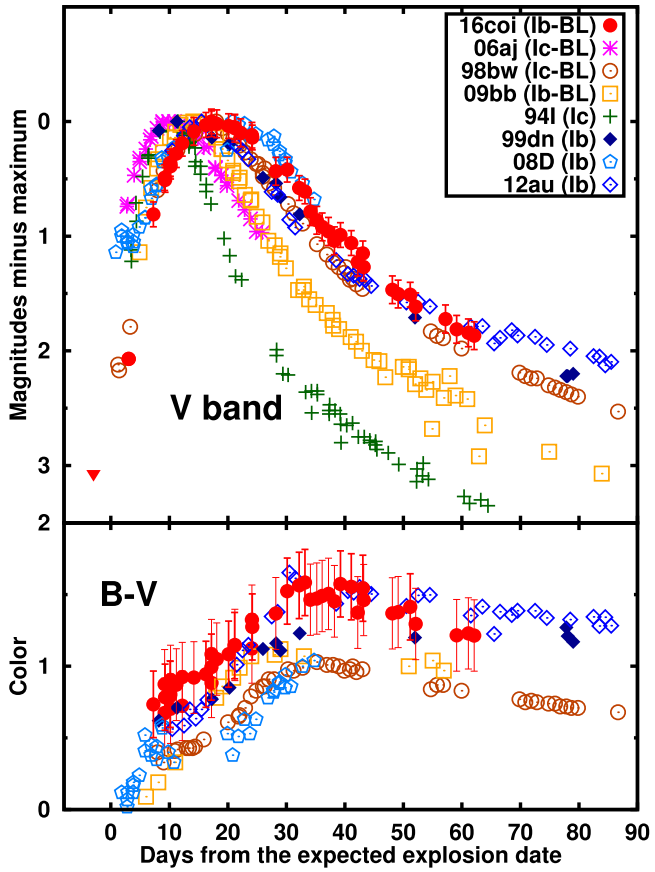

Figure 7. Top panel: the *V*-band light curve compared with those of SNe Ic-BL 1998bw (Clocchiatti et al. 2011), 2006aj (Ferrero et al. 2006), 2009bb (Pignata et al. 2011), a normal SN Ic 1994I (Richmond et al. 1996), SNe Ib 2008D (Modjaz et al. 2009), and 2012au (Takaki et al. 2013). The light curves are shown in magnitudes relative to the maximum. Bottom panel: the evolution of $B - V$ color compared with those of other SNe as in the top panel. Color excesses due to the Galactic and host galactic extinction were corrected for using the values reported in each reference.

Holoien et al. (2016), and this date is denoted as $t = 0$ throughout this paper. The *V*-band light curves reached their maximum magnitude at $t = 17$ days.

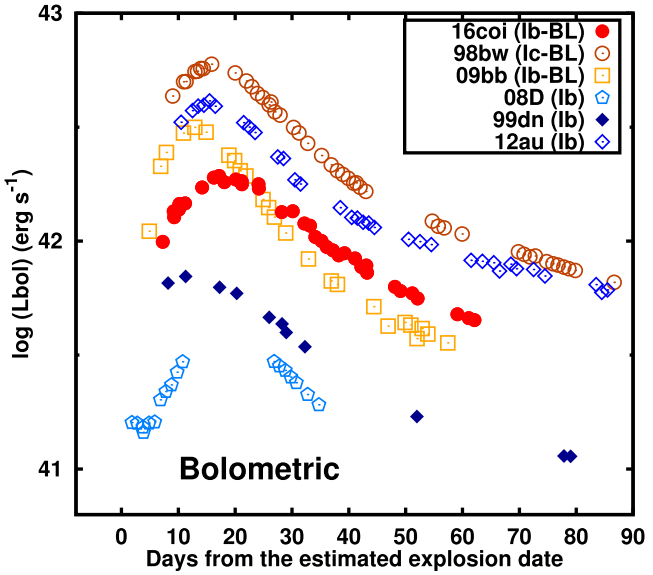

Figure 8. Quasi-bolometric light curve compared with those of other SNe. The bolometric light curves were constructed using optical (*BVRI*-band) light curves assuming that the optical fluxes are 60% of the total luminosity.

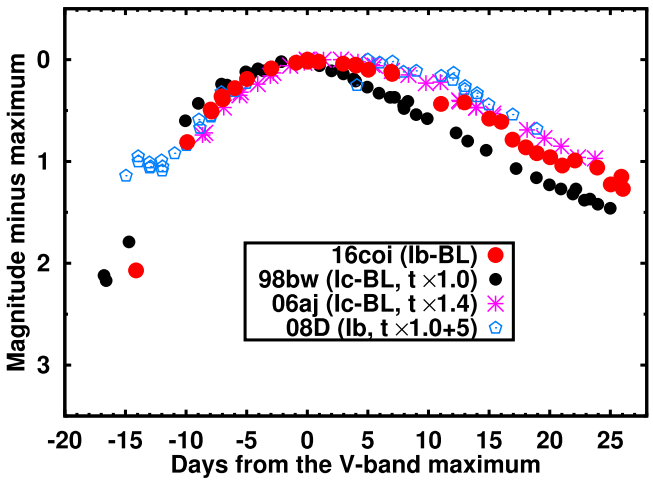

Figure 9. The *V*-band light curves compared with the stretched and shifted light curves of SNe 1998bw, 2006aj, and 2008D.

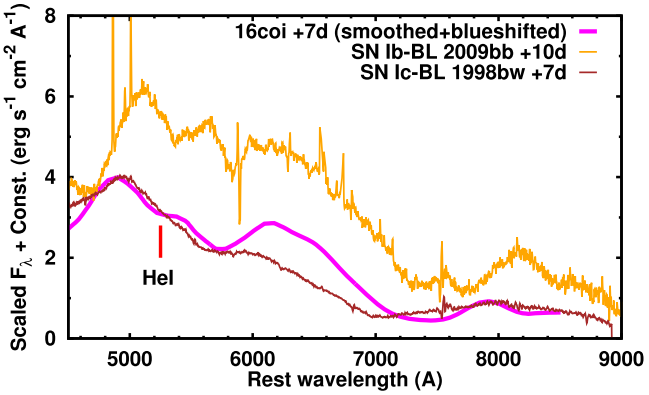

Figure 10. Blueshifted and smoothed spectrum of SN 2016coi compared with spectra of SNe Ic-BL 1998bw and 2009bb. The He I λ5876 feature was seen in SN 2016coi, but not in SN 1998bw.

The rising part of the light curves exhibited a slow evolution that was similar to those of SNe 1998bw, 2008D, and 2012au (see the upper panel of Figure 7). The estimated rise time of 17 days is similar to the 16.5 days of SN 2012au and 18 days of SN 1998bw, and slightly shorter than that of SN 2009bb. SN 2008D has a longer rise time than SN 2016coi. The rate of decline of SN 2016coi was also similar to those of SNe 1998bw, 1999dn, 2008D, and 2012au, but significantly slower than those of SNe 1994I and 2009bb.

The bottom panel of Figure 7 shows the evolution of $B - V$ color. The color excesses were corrected for using the values reported in each reference. The $B - V$ evolution of SN 2016coi was very similar to those of SNe 1999dn and 2012au, but different from those of SNe 1998bw, 2008D, and 2009bb. The color was always redder than those of SNe Ic-BL, and rather similar to those of SNe Ib.

To derive the absolute bolometric luminosity of SN 2016coi, the multiband light curve was integrated. The contribution of the optical emission to the total bolometric luminosity around the maximum date was assumed to be 60%. A distance modulus of $\mu = 31.18$ mag was adopted, which was taken from NED. For the comparison, the quasi-bolometric light curves of SNe 1998bw, 1999dn, 2008D, 2009bb, and 2012au were also constructed in the same manner. Figure 8 shows the quasi-bolometric light curves of these SNe.

The peak luminosity of SN 2016coi was estimated to be 3.2×10^{42} erg s^{-1}. It was substantially fainter than SNe 1998bw, 2009bb, and 2012au. It was more luminous than SNe 1999dn and 2008D. The ^{56}Ni mass of SN 2016coi was estimated to be $\sim$0.15 $M_{\odot}$, assuming that the rise time was 17 days and $\alpha = 1$ (Arnett 1982; Stritzinger & Leibundgut 2005). This ^{56}Ni mass was relatively small among SNe Ic-BL, while it is more consistent with normal SNe Ib.

4. Discussion and Conclusion

In this paper, we showed the results of our photometric and spectroscopic observations of SN 2016coi. He I lines were clearly identified in the spectra. Except for the presence of He I, the spectral features of SN 2016coi were similar to those of SNe Ic-BL. The line velocity as well as broad features of Si II and Ca II absorption lines were also similar to SNe Ic-BL. Pignata et al. (2011) pointed out that He I features were detected in spectra of SN Ic-BL 2009bb. The detection of possible He I features in NIR spectra was also reported for SN 2012ap (Milisavljevic et al. 2015). The detection of helium in these SNe means that they are classified as SNe Ib according to the definition. We suggest the classification of these SNe to be "Ib"-BL.

We estimate the kinetic energy and the total ejecta mass of SN 2016coi using the scaling method (see Sahu et al. 2008). Since the shape of the light curve of SN 2016coi was similar to the stretched light curves of SNe 2006aj and 2008D (see Figure 9), we use these objects as references. The timescale of the light curve of SN 2016coi was 1.4 times longer than that of SN 2006aj, while it is comparable to that of SN 2008D. The Si II line velocity of $\sim$15,000 km s^{-1} was similar to that of SN 2006aj and 1.6 times larger than the 9000 km s^{-1} of SN 2008D. Thus, by using SN 2006aj as a reference (Mazzali et al. 2006), the total ejected mass and the kinetic energy were estimated to be $M_{\rm ej} \sim 10\,M_{\odot}$ and $E_k \sim 3.0 \times 10^{52}$ erg. Similarly, by using SN 2008D as a reference (Tanaka et al. 2009), the kinetic energy and the total ejected mass were estimated to be $M_{\rm ej} \sim 10\,M_{\odot}$ and $E_k \sim 5.0 \times 10^{52}$ erg. The estimated ejecta masses and the kinetic energies were similar to those of GRB-SNe.

The presence of He in other BL SNe is of great interest. To study this possibility, we further smoothed and blueshifted the spectrum of SN 2016coi to match the absorption velocity and width to those of SN 1998bw (see Figure 10). We confirmed that the smoothed spectrum of SN 2016coi still shows a hint of the He I features, while this is not seen in the spectrum of SN 1998bw. Therefore, SN 1998bw does not have a similar amount of He. These considerations suggest that SN 2016coi (also SNe 2009bb and 2012ap) may belong to a different class of SNe from the prototype of BL SNe. This is in line with the finding by Modjaz et al. (2016), who concluded that SNe Ic-BL are He-free. There may be diversity among BL SNe in terms of helium content in the outer layer. A caveat is that it would also be possible that other BL SNe still contain the He layer, but the He lines are not strong in the absence of nonthermal excitation (e.g., Hachinger et al. 2012).

This work demonstrates the important role of observations in the very early phase for the identification of He in BL SNe. The He I absorption lines seen in SN 2016coi became very weak at $t = 15$ days, while the He I lines generally become stronger at later epochs for SNe Ib (Matheson et al. 2001). We speculate that the He I lines may have eluded detection due to the lack of pre-maximum early-phase spectra.

Our work has demonstrated the diversity of the outermost layer in BL SNe. The presence of He in BL SNe is indeed favorable to standard models of stellar evolution because it is difficult to remove all the helium layer from the progenitor in many models (Woosley et al. 1995; Yoon et al. 2010; Yoon 2015). The observed diversity must reflect the variety of evolutionary paths, but the exact origin is not yet understood. To understand the evolutionary paths to BL SNe and their variety, observations of more BL SNe from early phases will be important.

This work was supported by the Optical and Near-infrared Astronomy Inter-University Cooperation Program, and the Hirao Taro Foundation of the Konan University Association for Academic Research. This work was partly supported by the Grant-in-Aid for Scientific Research from JSPS (26800100, 15H02075, 15H00788). The work by K.M. is partly supported by WPI Initiative, Mext, Japan.

References

Akitaya, H., Moritani, Y., Ui, T., et al. 2014, Proc. SPIE, 9147, 4
Arnett, W. D. 1982, ApJ, 253, 785
Benetti, S., Turatto, M., Valenti, S., et al. 2011, MNRAS, 411, 2726
Bufano, F., Pian, E., Sollerman, J., et al. 2012, ApJ, 753, 67
Clocchiatti, A., Suntzeff, N. B., Covarrubias, R., & Candia, P. 2011, AJ, 141, 163
Elias-Rosa, N., Mattila, S., Lundqvist, P., et al. 2016, ATEL, 9090, 1
Ferrero, P., Kann, D. A., Zeh, A., et al. 2006, A&A, 457, 857
Filippenko, A. V. 1997, ARA&A, 35, 309
Foley, R. J., Papenkova, M. S., Swift, Brandon, J., et al. 2003, PASP, 115, 1220
Galama, T. J., Vreeswijk, P. M., van Paradijs, J., et al. 1998, Natur, 395, 670
Giovanelli, R., & Haynes, M. P. 1993, AJ, 105, 1271
Hachinger, S., Mazzali, P. A., Taubenberger, S., et al. 2012, MNRAS, 422, 70
Holoien, T. W.-S., Stanek, K. Z., Brown, J. S., et al. 2016, ATEL, 9086, 1
Iwamoto, K., Mazzali, P. A., Nomoto, K., et al. 1998, Natur, 395, 672
Kawabata, K. S., Jeffery, D. J., Iye, M., et al. 2002, ApJ, 580L, 39
Kawabata, K. S., Nagae, O., Chiyonobu, S., et al. 2008, SPIE, 7014, 4
Kotani, T., Kawai, N., Yanagisawa, K., et al. 2005, NCimC, 28, 755

Landolt, A. U. 1992, AJ, 104, 340
Matheson, T., Filippenko, A. V., Li, W., Leonard, D. C., & Shields, J. C. 2001, AJ, 121, 1648
Mazzali, P. A., Deng, J., Nomoto, K., et al. 2006, Natur, 442, 1018
Milisavljevic, D., Margutti, R., Parrent, J. T., et al. 2015, ApJ, 799, 51
Modjaz, M., Liu, Y. Q., Bianco, F. B., & Graur, O. 2016, ApJ, 832, 108
Modjaz, M., Li, W., Butler, N., et al. 2009, ApJ, 702, 226
Nagayama, T., Nagashima, C., Nakajima, Y., et al. 2003, Proc. SPIE, 4841, 459
Nomoto, K., Tominaga, N., Umeda, H., Kobayashi, C., & Maeda, K. 2006, NuPhA, 777, 424
Patat, F., Cappellaro, E., Danziger, J., et al. 2001, ApJ, 555, 900
Pignata, G., Stritzinger, M., Soderberg, A., et al. 2011, ApJ, 728, 14
Richmond, M. W., van Dyk, S. D., Ho, W., et al. 1996, AJ, 111, 327
Sahu, D. K., Tanaka, M., Anupama, G. C., Gurugubelli, U. K., & Nomoto, K. 2008, ApJ, 680, 580
Sakimoto, K., Akitaya, H., Yamashita, T., et al. 2012, Proc. SPIE, 8446, 73
Sako, S., Aoki, T., Doi, M., et al. 2012, SPIE, 8446, 6
Schlafly, E. F., & Finkbeiner, D. P. 2011, ApJ, 737, 103
Stritzinger, M., & Leibundgut, B. 2005, A&A, 431, 423
Takaki, K., Kawabata, K. S., Yamanaka, M., et al. 2013, ApJL, 772, L17
Tanaka, M., Maeda, K., Mazzali, P. A., & Nomoto, K. 2007, ApJL, 668, L19
Tanaka, M., Tominaga, N., Nomoto, K., et al. 2009, ApJ, 692, 1131
Thomas, R. C., Nugent, P. E., & Meza, J. C. 2011, PASP, 123, 237
Ui, T., Sako, S., Yamashita, T., et al. 2014, SPIE, 9147, 6
Valenti, S., Benetti, S., Cappellaro, E., et al. 2008, MNRAS, 383, 1485
Watanabe, M., Takahashi, Y., Sato, M., et al. 2012, Proc. SPIE, 8446, 84462O
Woosley, S. E., Langer, N., & Weaver, T. A. 1995, ApJ, 448, 315
Yamanaka, M., Maeda, K., Kawabata, K., et al. 2015, ApJ, 806, 191
Yamanaka, M., Maeda, K., Tanaka, M., et al. 2016, PASJ, 68, 68
Yaron, O., & Gal-Yam, A. 2012, PASP, 124, 668
Yoon, S.-C. 2015, PASA, 32, e015
Yoon, S.-C., Woosley, S. E., & Langer, N. 2010, ApJ, 725, 940